Research Square

Preprints are preliminary reports that have not undergone peer review.
They should not be considered conclusive, used to inform clinical practice,
or referenced by the media as validated information.

Vegetation cover shapes community structure and metabolic genetic potential of high- alpine soil microbiomes

Laureen S. Ahlers

laureen.ahlers@epfl.ch

École Polytechnique Fédérale de Lausanne

Massimo Bourquin

École Polytechnique Fédérale de Lausanne

Eduard Vico-Oton

École Polytechnique Fédérale de Lausanne

Gordanna Pistoletti Blanchet

École Polytechnique Fédérale de Lausanne

Anastasiia Kosolapova

École Polytechnique Fédérale de Lausanne

Gillian McClennen

École Polytechnique Fédérale de Lausanne

Romain Castro

École Polytechnique Fédérale de Lausanne

Beat Frey

Swiss Federal Research Institute WSL

Andrea Söllinger

UiT The Arctic University of Norway

Ianina Altshuler

École Polytechnique Fédérale de Lausanne

Research Article

Keywords: Alpine permafrost, alpine greening, soil microbiome, metagenomics, functional potential, greenhouse gas fluxes

Posted Date: August 10th, 2026

DOI: https://doi.org/10.21203/rs.3.rs-9790767/v1

License: This work is licensed under a Creative Commons Attribution 4.0 International License.
Read Full License

Additional Declarations: No competing interests reported.

Abstract

Background

Alpine permafrost-affected soils, particularly in the European Alps, remain poorly understood despite rapid warming and projected vegetation increase at higher elevations. We investigated how vegetation cover and physicochemical soil properties structure microbial communities across ten high-altitude alpine permafrost-affected sites.

Results

Soil parameters (pH, soil water content, temperature, and total C and N contents) varied significantly between sites and revealed pH and C:N ratio as key drivers modulated by vegetation cover, highlighting its indirect role in shaping soil environments. Microbial community composition differed significantly across sites, and functional gene profiles mirrored taxonomic patterns, indicating strong coupling between community structure and functional gene potential, without functional redundancy. Microbial abundance increased with vegetation cover, whereas taxonomic and functional gene diversity plateaued at intermediate vegetation cover, suggesting that the presence of vegetation primarily enhances microbial abundance rather than diversity. Genome-resolved metagenomics revealed a shift from generalist-dominated communities in barren soils to increased prevalence of specialist taxa in vegetated soils. Functional gene abundances, particularly for C cycling, were higher in vegetated soils, while N and S cycling gene potentials were associated with soil temperature and water content. A microcosm experiment measuring *ex situ* CO_2 and CH_4 fluxes from incubated summer soils, identified vegetated soils as modest CO_2 sources. Vegetated soils exhibited lower, pH and C:N ratio, shaping a more abundant microbial community with more specialist members and higher C cycling gene potential.

Conclusion

Overall, our findings indicate that alpine greening reshapes microbial communities via vegetation-mediated changes in soil properties, with implications for biogeochemical cycling and C emissions under climate warming.

Background

Anthropogenic climate warming accelerates permafrost degradation and often enhances greenhouse gas (GHG) fluxes by altering microbial activity and ecosystem processes[1]. While most permafrost research has focused on Arctic regions, alpine permafrost ecosystems remain comparatively understudied. Yet, Arctic soils differ substantially from alpine soils and make it difficult to infer knowledge on alpine soils from studying Arctic soils[2, 3]. Alpine high-altitude permafrost typically contains lower carbon (C) stocks, exhibits a thicker active layer, and features drier soils with steep

temperature and UV-radiation gradients due to altitude, resulting in amplified local warming effects[4, 5]. Most studies on alpine permafrost-affected soils have focused on the Tibetan Plateau, leaving a major knowledge gap regarding GHG fluxes in European permafrost-affected soils. Indeed, the European Alps are warming faster than the global average and experiencing rapid snow cover loss[6–9].

Alpine permafrost ecosystems are embedded within a highly heterogeneous landscape shaped by complex geological and glacial history[10]. The European Alps comprise a mosaic of crystalline and sedimentary bedrock, including carbonate- and silicate-dominated substrates, which strongly influence soil development, pH, buffering capacity, and inorganic C content[10–13]. In addition, repeated glacial advances and retreats have resulted in relatively young, shallow, and spatially heterogenous soils, often characterized by limited organic matter accumulation and strong local variability[14–16]. As a consequence, alpine permafrost-affected soils occur as spatially discontinuous “islands” across mountain ridges and peaks rather than as extensive, continuous bodies[17–19].

This landscape fragmentation likely imposes strong constraints on microbial community assembly through a combination of environmental filtering and limited dispersal among isolated habitats[20, 21]. Microbial communities in alpine permafrost-affected soils may therefore reflect both local adaptation to steep microclimatic gradients and historical contingencies related to soil formation and exposure[20, 21]. Compared to arctic lowland permafrost systems, which are often underlain by more continuous geological substrates, alpine environments provide a unique natural laboratory to examine how geological heterogeneity, topography, and spatial isolation interact to structure soil microbial communities[3, 20, 22–24]. Consequently, sampling across multiple sites is essential to capture this variability and to avoid site-specific bias when assessing microbial diversity and ecosystem function in alpine permafrost ecosystems.

Alpine permafrost-affected soils are typically dominated by bacteria, with smaller contributions from fungi, archaea, and microeukaryotes[25, 26]. In the Tibetan Plateau, soil moisture, the C:N ratio and pH, were identified as major drivers of microbial community composition[27]. However, in Arctic Soils, pH was found as the main driver of bacterial communities, with organic C (TOC) and soil moisture being less important[28]. The vegetation effect on soil chemistry in Tibetan Plateau shows that sparsely vegetated soils exhibit higher C:N ratios and pH, but lower moisture, total C, and N, compared to soils with denser vegetation extent[27]. Vegetated, nutrient-rich soils generally support higher microbial diversity and enhance microbial abundance through rhizosphere-associated resources and labile C inputs[27].

Several studies showed that ongoing climate warming causes an upward shift of vegetation belts, known as “alpine greening”[9, 29, 30], likely affecting microbial communities and their contributions to C and N cycling[31]. A similar process is occurring in Arctic regions with a vegetation expansion into higher latitudes[32–34]. In permafrost-affected environments, thaw-induced increases in substrate availability and root-derived C inputs can stimulate microbial production of C active enzymes (CAZymes) thereby accelerating the decomposition of previously frozen or physically protected organic matter[1, 35, 36].

CAZymes are extracellular enzymes, which catalyze the synthesis and breakdown of complex plant-derived polymers across multiple functional classes[37]. Root exudates may further enhance this process through microbial priming effects, increasing enzyme expression and overall respiration rates[38]. The abundance and diversity of CAZyme genes therefore provide insights into the microbial capacity for organic matter turnover and C mobilization in soils[39–41]. CAZyme gene profiles represent functional indicators of microbial decomposition potential and offer a mechanistic link between environmental change, microbial metabolism, and CO_2 fluxes[42]. Experiments simulating root exudate release in active layer soils and permafrost show elevated microbial respiration and reduced diversity[38]. Moreover, access to labile C allows microorganisms to produce CAZymes, further influencing microbial activity. This process establishes a positive feedback loop in which microbial respiration may exceed CO_2 uptake via photosynthesis[43–45]. In Arctic systems, permafrost thawing generally increases microbial activity and GHG emissions[43, 44]. However, current knowledge of microbial taxa driving C and nitrogen (N) cycling and resulting GHG fluxes (CO_2, CH_4, and N_2O) largely stems from Arctic permafrost studies[35, 46, 47]. While alpine greening is recognized as an important factor, quantitative studies linking vegetation shifts to microbial-mediated GHG fluxes in the European Alps are currently lacking[9]. Evidence from the Tibetan Plateau suggests increased CO_2 emissions in alpine permafrost regions[48, 49], yet the sink–source function of European high-altitude permafrost remains uncertain due to concurrent increases in plant productivity[50]. Investigating microbial community compositions and their functional potential in these threatened and already changing environments is crucial for understanding microbial adaptations to extreme alpine conditions and their responses to alpine greening.

In this study, we evaluate how environmental variables, including vegetation cover, pH, C:N ratio, soil water content, and soil temperature shape soil microbial communities and their functional roles in CO_2 and CH_4 fluxes across high-altitude permafrost-affected sites in the European Alps.

We hypothesize that i) the taxonomic composition of soil microbial communities in alpine permafrost-affected soils is primarily structured by vegetation cover and associated physicochemical soil variables, where vegetated soils host more diverse and functionally versatile microbial communities, while barren soils harbor less diverse taxa, ii) soils across alpine permafrost sites may contain taxonomically different compositions that will be functionally redundant and iii) the metabolic potential of microbial communities, particularly genes involved in C and N cycling, is linked to soil properties, reflecting distinct functional strategies between vegetated and barren soils.

To test these hypotheses, we conducted an integrated field and laboratory study across ten high-altitude permafrost-affected sites in the European Alps with various vegetation cover extents (0.1–20% average coverage, Fig. 1B). We combined metagenomic sequencing, soil physicochemical analyses, cell abundance estimates, and controlled microcosm incubations to link microbial community composition, abundance, and functional gene potential with environmental variation and GHG fluxes. Specifically, we characterized spatial patterns in microbial diversity and taxonomic composition across vegetation and soil physicochemical gradients, identified key environmental drivers shaping the functional gene

potential of microbial communities involved in C and N cycling, and quantified *ex-situ* soil CO_2 and CH_4 fluxes to evaluate how microbial processes translate into soil function.

Methods

Field sites and soil sampling

The selected study area is located in the Swiss Alps and includes 10 high-altitude soil sites (2500–2990 m a.s.l.; Fig. 1). Permafrost-affected sites were selected based on alpine permafrost extent, predicted by the “alpine permafrost index map” (APMI, University of Zurich and PermaNET) and the “permafrost and ground ice map” (Swiss Federal Institute for Forest, Snow and Landscape Research WSL) [17, 18]. The lithology of the underlying bedrock was assessed with the “Lithological map of Switzerland 1:500000” (Federal Office of Topography swisstopo, Georesources Switzerland Group) and the ecoregion of the sites was investigated with the map “Forest ecoregions” (Federal Office for the Environment FOEN)[51, 52].

Soil sampling was conducted in Summer 2023 (June 9 – July 19) with five replicates per site, sampled at 0 to 5 cm depth (topsoil) and 5 to 15 cm depth (lower soil layer) for comparison of soil physicochemical properties (n = 30) and microbial communities (n = 90). *In-situ* soil temperature was measured at both depths. The sampled soils were homogenized and transported to the lab on ice where they were frozen at -20°C prior to further analysis. The vegetation cover was quantified in percent canopy cover of live green vegetation in photographs taken at sampling timepoint using the Canopeo App[53]. See Supplementary file S1-2 for more information about collected metadata.

The sites MY1 and MY2 were initially sampled as one site but soil chemical analysis of the biological replicates revealed a significantly lower pH in the biological replicates d and e (now MY2) related to lower altitude and higher vegetation cover (Welch’s Two Sample t-test, $p < 0.01$, $n = 8$; see Supplementary file S3). Thus, they were treated as separate soil sites (Fig. 1B).

Soil physicochemical parameters

Gravimetric water content (GWC) was determined by drying 2 g of frozen soil at 100°C for 24 h and subtracting dry weight from wet weight. GWC was expressed as percent moisture per gram of wet soil and will from here on be referred to as soil water content (SWC).

$$GWC\,(\%) = \frac{wetsoilweight\,(g)\text{-}drysoilweight\,(g)}{wetsoilweight\,(g)} \times 100$$

To determine soil pH, 2 g of frozen soil were mixed with 5 mL 0.05 M $CaCl_2$ solution and pH was measured with a Orion Lab Star PH111 pH/mV meter (Thermo Fisher Scientific, WA, USA). Total carbon (TC), total nitrogen (TN) and total hydrogen (TH) contents were quantified from dried (30°C for 4 h),

sieved (2 mm) and ground soil using a Thermo Finnigan Flash EA 112 CHSN elemental analyzer (Thermo Fisher Scientific, WA, USA) at the Institute for Earth Science, University of Lausanne. Further, for quantification of total organic C (TOC) the soil was acidified with 2x 50 µL 1 M HCl to eliminate inorganic C, incubated overnight, then acidified again with 2x 50 µL 1 M HCl and dried (4 h, 100°C) before analysis with the Thermo Finnigan Flash EA 112 CHSN elemental analyzer (Thermo Fisher Scientific, WA, USA). Ion concentrations of sodium (Na), chloride (Cl), calcium (Ca), potassium (K), ammonium (NH), nitrate (NO), magnesium (Mg) were determined using a portable nutrient analyzer IMACIMUS10 (NT Sensors, Tarragona, Spain) from 3 g dried (30°C for 4 h), sieved and ground soil in 20 mL deionized water.

$$soilnutrients\,(mg/\mathrm{g}) = \frac{water\,(L)}{soil\,(g)} \times\ ionconcentration\,(mg/L)$$

Ex-situ *GHG rate potential of the soils*

For a microcosm experiment, soil from three replicates of each site were thawed and approximately 10 g of each soil layer, topsoil and lower layer, were weighed into 250 mL glass bottles to allow maximum gas headspace and capped with sterilized aluminum foil. The created soil microcosms were incubated in the dark at the average sampling temperature of 12.5°C. After 72 h incubation time, CO_2 and CH_4 concentrations were measured with the portable trace gas analyzer LI-7810 (LiCor, Lincoln, NE, USA). Gas concentration data (ppm CO_2 and CH_4) were processed in R to calculate oxidation and production rates based on the ideal gas law.

$$n\,(mol) = \frac{P\,(\mathrm{bar})\ *\backslash{:}V\,(L)}{0.08314(L\cdot bar\cdot K\square\square\cdot mol\square\square)*\backslash{:}T\,(K)}$$

For each measurement, the headspace temperature was converted to Kelvin, and the total headspace volume was calculated as the sum of the incubation headspace (L), analyzer dead volume, and tubing volume. The total number of moles of gas in the headspace was then estimated using the ideal gas law (P = 1 bar; R = 0.08314 L·bar·K⁻¹·mol⁻¹). CO_2 and CH_4 concentrations were converted to µmol by multiplying the measured mole fraction by the total headspace molar content (including headspace volume, dead volume, and tubing volume). For both gases, time series were analyzed using a linear model of µmol versus time. Slopes were obtained for each sample and gas species, converted to per-minute rates, and then scaled to per-hour oxidation rates (µmol g⁻¹ h⁻¹) by normalizing by soil fresh weight.

Flow cytometry for cell enumeration

Cells were detached from the soil matrix by a modified protocol based on Gorniak *et al* [54] with 1 g frozen soil mixed with 9 mL filtered PBS that was horizontally shaken at 120 rpm for 2 h at 10°C to detach cells. Cells were fixed using 100 µL formaldehyde and 900 µL soil slurry. For separation of cells from the debris 1 mL fixed soil slurry was placed on 0.5 mL Histodenz solution (1.3 g mL^{-1}) and

centrifuged for 90 min following the centrifuge density gradient method based on Frossard *et al* [55]. DNA staining was conducted in technical triplicates by mixing 2 µL SYTO®13 (50 µM) with 198 µL cell supernatant and incubating for 15 min in the dark. Samples were analyzed in a NovoCyte Flow cytometer (ACEA Biosciences, CA, USA) at a flowrate of 14 µL min^{-1}. Unstained soils were used as a cell positive but unstained control to determine the soil autofluorescence threshold at each site so that events above the threshold could be considered microbial cells. Negative controls without soil slurry yielded lower counts that subsequently were subtracted from the sample counts.

Nucleic acid extractions and sequencing

DNA was extracted from soil samples along with negative extraction controls with the DNeasy PowerSoil Pro kit (Qiagen, Hilden, Germany) adjusted to low biomass samples. Soil mass was increased to 1 g and cells were lysed in a Precellys 24 homogenizer (3 x 30 sec at 5500 rpm, 30 sec pause) (Bertin Technologies, Montigny-le-Bretonneux, France). The final DNA extract was eluted in two 50 µL washes using DNase free water and if necessary, vacuum concentrated (30°C, 1 h). For low-biomass soils, where extraction from 1 g of soil did not yield sufficient sequencing amounts (< 0.1 ng DNA μL^{-1}), the protocol was further adjusted. Soil mass was increased to 3.5 g and lysis was performed in 7 mL Soil Grinding SK38 (Bertin Technologies). Supernatants were pooled from two 7 mL tubes per sample (total of 7g soil) and subsequent reagent volumes were proportionally scaled to the initial soil volume.

Metagenomic libraries were prepared for short read sequencing with the Illumina DNA Prep Kit (Illumina, CA, USA) for short fragments following the manufacturers protocol and sequenced on AVITI (Element Biosciences, CA, USA) at the Gene Expression Core Facility (EPFL, Switzerland).

Sequence data processing

Raw Illumina paired-end reads were quality trimmed and adapter filtered using Trim Galore (v0.6.10) with default settings in paired-end mode, that perform automatic adapter removal and quality filtering (q > 20) including FastQC quality assessment[56]. Negative control samples were included in the quality assessment and did not show signs of contamination. They were thus excluded from downstream analyses.

Metagenomic assemblies were generated from all samples using MEGAHIT (v1.2.9) with the meta-large preset and a multi-k-mer strategy (k = 27–127, step size 10) that improves assembly continuity in high-diversity microbial communities[57, 58].

Contigs shorter than 1,500 bp were removed using SeqKit (v2.1.0)[59]. Short reads were mapped against the filtered assembly using CoverM (v0.7.0) with contig mode and standard parameters[60]. Read alignment was performed using BWA-MEM2 (v2.2.1) [61].

Metagenome-assembled genomes (MAGs) were reconstructed using three independent binning algorithms: MaxBin2 (v2.2.7), MetaBAT2 (v2.17), and Rosella (v0.5.3)[62–64]. All binning tools were run with a minimum contig length threshold of 1.5 kb. MaxBin2 uses tetranucleotide frequencies and coverage-based Expectation–Maximization clustering[63]. MetaBAT2 performs probabilistic distance estimation based on sequence composition and differential coverage[62]. Rosella incorporates coverage profiles and sequence composition for binning refinement[64].

Bins from all tools were integrated and refined using Binette (v1.1.1): Binette performs dereplication, scoring, and refinement across multiple binning outputs using default parameters (filtering out bins with a completeness below 40% based on Checkm2 assessment within Binette)[65]. For MaxBin2, trimmed mean coverage values were additionally calculated to generate per-sample abundance profiles for downstream binning[63]. Genome quality (completeness and contamination) was assessed using CheckM2 (v2.2.1) with the UniRef100-based database (uniref100.KO.1.dmnd)[66]. Galah (v0.4.2) was used for dereplication with an ANI threshold of 99% to define strain-level clusters resulting in individual clusters for each bin[67].

Further, taxonomic annotation of the bins was carried out with GTDB-tk (v2.4.1) and of contigs with Kraken2 (v2.1.6) with subsequent CheckM2 for quality assessment[66, 68, 69]. For functional gene annotation eggnog-mapper used prodigal to predict gene coding sequences with the “--itype metagenome” argument (v2.1.12) [70]. MMseq2 (“search”) was used to obtain amino acid sequences for comparison to the Compiled Greening lab metabolic marker gene databases[71, 72]. Tiara (v1.0.3) was used to find eukaryote contigs that were cross-referenced with Kraken2 outputs, subsequently we used absolute coverage data for ratio calculation of prokaryotic:eukaryotic reads across site [73]. See Supplementary information for scripts used for metagenome processing and binning.

Data and Statistical Analyses

We used Rstudio v2025.9.0.387 (rstudio.com) and R (r-project.org) v4.5.0 and to analyze the data, perform statistical tests, and graphically display the results with R packages “tidyverse” (v.2.0.0), “cowplot” (v1.2.0), “ggpubr” (v0.6.2), “ggplot2” (v4.0.1)[74–76]. See Supplementary file S4-25 for details on statistical tests and analysis.

Statistical analysis of environmental parameters

Relationships among environmental and soil physicochemical variables were evaluated using pairwise Spearman correlation analysis. Spearman correlation coefficients (rho) and corresponding *p*-values were computed with corr.test() from the R package “psych” (v2.5.6), applying the Benjamini–Hochberg (BH) false discovery rate (FDR) correction to account for multiple testing[77]. Only statistically significant correlations (adj. $p < 0.05$) were retained for plotting.

To explore patterns in soil physicochemical soil properties, all variables were transformed according to their best normalization using the R package “bestNormalize” (v1.9.1) [78]. A principal component analysis (PCA) was performed based on a Euclidean distance matrix using prcomp() from the R package “stats” on the scaled data (scale = TRUE) to visualize differences among sites and soil depths[74]. To assess which environmental variables significantly explained variation in the PCA ordination, we applied vector fitting with envfit() from the R package “vegan” (v2.7-2) using 999 permutations and then retained only significant variables after BH correction (adj. $p < 0.05$) [79]. Relationships between inter-sample differences and soil properties were tested using permutational multivariate analysis of variance (PERMANOVA) with adonis2() from “vegan” based on Euclidean distance matrix (999 permutations)[79].

Results

All alpine permafrost-affected sites varied in altitude, vegetation extent, and basic soil physicochemical parameters (Fig. 1).

The underlying bedrock (lithology) varied across sites, and the ecoregions corresponded to either the continental Alps or the northern pre-Alps (Fig. 1B). Altitude ranged from 2485 m a.s.l. to 2941 m a.s.l on plateaus or north facing slopes with permafrost prediction indexes of “patchy permafrost” and “likely extensive permafrost” (Fig. 1B; Supplementary Table S1) (south facing slopes tend not to be permafrost-affected). The average vegetation cover was as low as 0.1% in the rockier sites and reached up to 20.2% in the most vegetated site. More vegetated soils such as BN, MY2, SF (vegetation extent > 10%) generally had an acidic pH, higher total organic carbon (TOC), and total nitrogen (TN) contents, while barren soils such as DS, MF, BN (vegetation cover extent < 1%), overall were less nutrient-rich, and had a higher pH (neutral). Soil water content (SWC) across the sites ranged from 6.9% to 36.8%. Site BN exhibited the highest vegetation cover (20.2 ± 17.5%) in combination with highest soil water content (36.8 ± 16%), TOC (6.03 ± 3.46%), TN (0.36 ± 0.22%) and the lowest pH (3.9 ± 0.1). The highest C:N ratios were characteristic of the barren soils (66.5–130.2).

Environmental Soil Variables

Relationships between environmental and soil physicochemical parameters were explored with pairwise correlation (Spearman’s correlation, n = 51) and a PCA (Fig. 2A; Supplemental Figure S1).

Among the assessed variables, altitude was weakly but significantly correlated with microbial cell numbers, pH, TOC and vegetation cover and exhibited a strong negative correlation with *ex-situ* CO_2 rates. TOC and total hydrogen (TH) increased with higher vegetation cover, while pH was lower at higher vegetation extents underlining the role of vegetation for nutrient availability in high-altitude soils. Microbial cell numbers increased with vegetation cover and lower pH. Notable, vegetation cover was not significantly correlated with SWC and soil temperature. Soil temperature was colder in the lower soil layer compared to the topsoil layer, while higher temperatures were correlated with lower SWC. For Spearman’s rho and adjusted p-values see Supplementary file S4-7.

Environmental and physicochemical soil properties differed significantly across alpine permafrost-affected soil sites and across the two sampled depths (Fig. 2B; PERMANOVA, adj. $p < 0.001$, $n = 55$). While the top-soil layer appeared most influenced by soil temperature, followed by pH, Ca, TOC and SW, the lower-soil layer was more affected by the chemical parameters than temperature (Supplemental Figure S1).

Microbial Community Characteristics

Beyond differences in physicochemical soil properties, the microbial community composition of the alpine permafrost-affected soils were explored using shotgun metagenomics sequencing with cell number normalized abundance (Fig. 3). The assembly of reads produces 600,841 contigs with an average length of 2,679.4 bp, ranging from 1,500 bp (filter threshold) to 339,970 bp and an N50 value of 2,601 bp. Of all sequencing reads, 82.7% mapped to assembled contigs, indicating the assembly captured most of the sequenced community. Negative control samples yielded fewer reads and mostly non-soil taxa.

All samples were dominated by Bacteria, followed by Archaea, Eukarya, and viruses (Supplementary Figure S2A; Supplementary file S8). The dominant taxa across sites were Actinomycetota and Pseudomonadota (Supplementary Figure S3). The ratio of prokaryotes:eukaryotes was lower in barren than vegetated soils, but this difference was not significant (Supplementary Figure S2B). We recovered 243 metagenome-assembled genomes (MAGs), of which 22 were classified as high quality (≥ 90% completeness, ≤ 5% contamination) and 171 as medium quality (≥ 50% completeness, ≤ 10% contamination). MAG completeness ranged from 39.2% to 100%, with contamination values between 0.03% and 30.9%. The 243 MAGs captured 42.3% of the total reads, showing they represent most of the microbial community. Three MAGs were classified as Archaea of the family Nitrososphaeraceae.

Site and soil depth had a significant effect on microbial community composition (PERMANOVA, adj. $p < 0.001$, $n = 70$), indicating site-specific depth effects (Fig. 3A). The taxonomical clustering of samples revealed clear grouping of sites according to vegetation presence; barren soils formed distinct clusters from soils with higher vegetation extents. NMDS ordinations of the taxonomic composition based on the full metagenome (Fig. 3A) and based on MAGs (Supplementary Figure S4) were consistent with each other, indicating the suitability of our MAGs for the taxonomic representation of the whole community. Additionally, full lengths 16S rRNA gene amplicon-based sequencing corroborated these site patterns (Supplementary Figure S5).

Functional profiles differed significantly between sites and depths within sites (PERMANOVA, adj. $p < 0.001$, $n = 70$). Further, functional profiles mirrored taxonomic site patterns and indicate that metabolic potential aligns with taxonomic composition (Fig. 3B). Across all NMDS analyses, important environmental drivers included pH, vegetation cover, TOC, TN and C:N (Supplementary file S9-11).

Alpha diversity (Shannon index based on MAG abundances) ranged from 3 to 5.25, with barren soils having lower diversity while medium vegetated sites harbored the most diverse communities (Fig. 3C).

Alpha diversity was significantly different across sites (Kruskal-Wallis, adj. $p < 0.001$, $n = 70$), while soil depth did not affect diversity significantly within sites (Supplementary file S12). Further, functional gene diversity based on KO terms showed a similar pattern to taxonomic alpha diversity: barren sites had lower functional diversity than vegetated soils with a plateau at medium vegetation cover (Supplementary Figure S6; Supplementary file S13).

Cell numbers per sample ranged significantly and considerably from 5 to 2149 cells g $soil^{-1}$, with barren soils containing extremely low numbers of cells and vegetated soils representing higher numbers of cells (Kruskal-Wallis, adj. $p < 2.2e\text{-}16$, $n = 210$; Fig. 3D). Soil depth exhibited no significant differences in cell numbers within sites (Supplementary file S14).

Vegetation impact on taxonomical abundance and diversity

To investigate the impact of vegetation cover on microbial taxonomy and alpha diversity, we used differential abundance analysis of MAGs and generalized additive models (GAMs) across vegetation cover (Fig. 4). A total of 67 MAGs, spanning six phyla and 29 families, showed significant log fold changes (LFC) across vegetation cover (Fig. 4A; Supplementary file S15). These MAGs were distributed across phyla with distinct response patterns: Pseudomonadota, Acidobacteriota, and Chloroflexota MAGs showed both positive and negative responses to increasing vegetation cover. In contrast, Actinomycetota and Verrucomicrobiota contained significant MAGs with only positive responses, while significant Gemmatimonadota MAGs only showed negative responses to vegetation extent (Fig. 4A; Supplementary file S15).

GAMs revealed a significant nonlinear relationship between vegetation extent and alpha diversity as Shannon diversity increased with vegetation extent up to intermediate levels, after which the trend stabilized (Fig. 4A). The model explained 32.8% of the deviance and the smooth term was significant ($p < 3.39e\text{-}06$), indicating that vegetation extent is a very important predictor of microbial community diversity across the sites (Fig. 4B; Supplementary file S16).

An analysis of generalist and specialist MAGs (see Methods, "*Generalist vs. specialist MAG classification*" and Supplementary file S17) revealed that the relationship between specialist:generalist ratio and vegetation cover was similar to the alpha diversity pattern, with an initial increase of specialist:generalist at low vegetation cover and a stabilizing trend at intermediate levels (Fig. 4C). This trend was consistent across all niche breadth definitions tested (Supplementary Figure S7), demonstrating that it is not driven by methodological assumptions. The model explained 60.3% of the deviance and the smooth term was significant ($p < 2e\text{-}16$; Supplementary file S18). These results showed that specialist MAGs are more abundant at higher vegetation covers, while barren soils are closer to a specialist:generalist equilibrium. Notably, the barren site DS exhibited the lowest specialist:generalist and lowest diversity at low, but not the lowest vegetation cover.

Functional genetic potential of permafrost-affected soils

We compared ten alpine permafrost-affected sites regarding their metabolic potential and ecosystem function using gene abundances normalized to cell numbers and generalized additive models (GAMs) to investigate the effect of soil parameters on functional gene abundances (Fig. 5).

The abundance of marker genes for C, N and S cycling, trace gas cycling pathways of CH_4, CO and H_2, and metal electron transfer revealed an overall higher gene abundance in vegetated sites compared to barren sites and highlights CO, H_2 and C cycling as the most abundant metabolic pathways (Fig. 5A, Supplementary file S19). Notably, barren sites exhibited the lowest marker gene abundance in CH_4 oxidation.

Setting a stronger focus on C cycling related genes, we investigated the gene abundance of carbohydrate active enzymes (CAZymes). We found that the most abundant CAZyme class encoding genes across the study were glycoside hydrolases (GH) and glycosyltransferases (GF) and the most abundant genes encoding for C degradation were related to the plant substrates starch, cellulose and hemicellulose (Supplementary Figure S8; Supplementary file S20-21).

CAZyme classes for plant polymer degradation genes were driven by vegetation cover, more than soil temperature and SWC (Fig. 5B), with similar patterns observed in CAZyme abundance associated with the degradation of starch, cellulose, and hemicellulose (Fig. 5C,D). GH and GF gene abundance increased significantly with vegetation extent ($p = 0.00437$), while trends with SWC and soil temperature were non-significant (Fig. 5B). The model explained a large proportion of the deviance (43.6%). Gene abundances of starch and (hemi-)cellulose degrading enzymes revealed a significant relationship with vegetation extent ($p = 0.00329$, $p = 0.0097$) with increasing abundances at higher vegetation extents (Fig. 5C,D), while the smooth terms for SWC and soil temperature were nonsignificant. The model for starch degradation explained 27.7% and the model for hemi- and cellulose 19.2% of the deviance. Overall, gene abundances for plant substrate degrading enzymes increased significantly with increasing vegetation extent, whereas SWC and soil temperature played a lesser role (Supplementary file S22).

Moreover, gene abundances of the lithotrophic pathways S, N, CO, CH_4 and H_2 cycling were driven significantly by vegetation cover (Supplementary Figure S9; Supplementary file S23), suggesting that vegetation cover impacts the metabolic potential of European alpine permafrost-affected soils more importantly than soil temperature or SWC.

CO_2 and CH_4 fluxes from soil microcosms

GHG contributions of alpine permafrost-affected soil microcosms were very low and exhibited high variability between replicates (Fig. 5E). CO_2 emissions ranged from − 0.0058 to 0.697 µmol g^{-1} h^{-1}. Notably, only site BN with the highest vegetation extent showed significant differences to the barren soil site PM (Kruskal-Wallis, $p = 0.0122$, $n = 28$; *post-hoc* Dunn test, adj. $p = 0.0436$). CH_4 rates spread across negative (CH_4 oxidation) and positive values (CH_4 emission), ranging from − 2.68e-04 to 1.63e-04 µmol g^{-1} h^{-1}. The strongest CH_4 oxidation occurred in one biological replicate of the vegetated site BN, but no statistically significant differences were present (Supplementary file S24-25).

Together, these results suggest that vegetation is a key factor shaping both microbial community composition and ecosystem function in alpine permafrost-affected soils.

Discussion

In our study, alpine permafrost-affected soils differed in physicochemical properties, microbial community composition, and functional potential. Vegetation extent correlated with multiple soil properties, underscoring its role in structuring the soil environment. While microbial abundance increased with vegetation cover, taxonomic and functional diversity plateaued at intermediate levels, indicating that vegetation primarily enhances abundance rather than diversity. Furthermore, community composition shifted from generalist-dominated in barren soils to more specialist taxa in vegetated soils, likely reflecting adaptation to plant-derived substrates[42]. Functional gene abundances for C cycling and lithotrophic pathways were higher in vegetated soils.

Vegetation as a structuring force in alpine permafrost soils

Our results demonstrate that alpine permafrost-affected soils are strongly structured by physicochemical gradients, with pH and C:N ratio emerging as key drivers of microbial community composition and functional potential. These gradients were, however, closely associated with vegetation cover, highlighting vegetation as a powerful modifier of soil environments[86]. Rather than acting solely as a direct biotic driver, vegetation appears to restructure microbial communities primarily through plant–soil feedbacks that alter substrate availability, nutrient pools, and buffering capacity[86].

Vegetated soils exhibited lower pH and C:N ratios and higher microbial abundance compared to barren soils[36, 87–89]. Similar vegetation-mediated shifts in soil chemistry have been reported for alpine permafrost regions on the Tibetan Plateau, where sparsely vegetated soils display higher pH and C:N ratios but lower total C and N contents[27, 90]. In the active layer alpine permafrost of the Tibetan plateau, pH affected soil microbial community composition as well as C recalcitrance[91]. In Arctic systems, pH has been similarly identified as a dominant predictor of bacterial community structure, whereas moisture and organic C play more variable roles[28].

Qualitative assessment of plant species composition was beyond the scope of this study; instead we focusing on quantitative measurements of vegetation cover (% coverage), as vegetation cover and absence are likely more influential than composition at the low-vegetation end of the gradient (i.e. between barren soil and sparse plant patches)[92].

Importantly, alpine permafrost-affected soils in the European Alps are spatially fragmented and geologically heterogeneous[10–13, 17–19]. Vegetation may therefore operate both as a driver and as a proxy: it reflects underlying bedrock- and topography-driven edaphic conditions while simultaneously modifying them through litter input, root exudation, and rhizosphere processes[31, 86]. Disentangling these effects remains challenging and requires manipulative vegetation experiments or longitudinal monitoring across greening gradients. A study on rock microbiomes in an Arctic dessert found that the

microbial community was strongly related to rock types[93] with implications for the heterogeneity of the underlying bedrocks being reflected in the microbiome.

From barren to vegetated soils: restructuring of microbial community assembly

Microbial communities differed significantly across the alpine permafrost-affected sites, with barren soils clustering distinctly from vegetated soils based on beta diversity. This separation along the vegetation gradient suggests strong environmental filtering, where shifts in pH, C availability, and nutrient stoichiometry select for different taxonomic assemblages[94, 95]. Comparable patterns have been observed in alpine glacier forefields and early-successional alpine soils, where microbial communities transition from stress-tolerant pioneers to more specialized heterotrophic assemblages as organic matter accumulates[21, 89, 96, 97].

Metagenome-resolved analyses revealed that barren soils were enriched in generalist MAGs, whereas vegetated soils contained more specialists. Generalists are defined as exhibiting broad environmental tolerances and occurring in many habitats, while specialist having narrow environmental tolerances and being found in a limited number of habitats [98, 99]. The consistency of specialist–generalist patterns across multiple niche breadth metrics suggests that the observed shift reflects a genuine ecological transition rather than an artefact of metric choice. This robustness strengthens the inference that vegetation development promotes taxa with narrower ecological distributions, likely associated with plant-derived resource specialization.

Our barren soils were dominated by taxa with broad ecological distributions, whereas vegetated soils harbored an increased prevalence of specialist taxa. The shift towards specialist taxa in vegetated soils likely reflects niche diversification under greater substrate heterogeneity[100]. In exposed, nutrient-poor barren soils, generalists capable of tolerating desiccation, UV stress, and fluctuating temperatures may persist due to metabolic flexibility and stress resilience[101, 102]. Vegetation establishment stabilizes microclimatic conditions, increases organic inputs, and creates rhizosphere-associated niches[96, 100], thereby likely enabling specialist taxa to proliferate in permafrost-affected soils. We acknowledge the limitations of determining specialists and generalists along a single niche axis despite being exposed to complex soil environments[103].

Such patterns are consistent with ecological succession theory, where increasing resource availability promotes niche partitioning and specialization[104, 105]. Under ongoing alpine greening, taxa adapted to oligotrophic, mineral soils may decline, whereas copiotrophic and plant-associated taxa may expand. Differential abundance analyses in our dataset support this interpretation and identify candidate “winner” and “loser” lineages: families of the Actinomycetota, Verrumicrobiota and Chloroflexota mostly benefit from vegetation increase, while families of the Gemmatimonadota experience a decrease with vegetation increase. In desert environments and rocks, Actinomycetota and Chloroflexota, taxa with adaptations to dryness and high UV radiation, were found as the dominant taxa [93, 101].

Actinomycetota are pioneers of colonization in early soil systems and are able to prevail as generalists under changing conditions[100, 106]. In high-altitude shrub ecosystems on the Tibetan Plateau, Verrucomicrobiota were identified as one of the most abundant phyla[107]. Similarly, in arcto-alpine environments, Verrucomicrobia have been found to dominate the soil communities associated with pioneer plants colonizing harsh mineral soils[108]. Verrucomicrobiota appear to form strong associations with alpine vegetation, benefiting from the rhizosphere and playing a key role in the functional stability of these high-altitude ecosystems.

On the contrary, certain microbial taxa might suffer from vegetation increase. Following revegetation in a semi-arid desert mining area, a study found that shrubland plots were depleted of Gemmatimonadota[109], that were classified as K-strategists, which were outcompeted by r-strategists as vegetation and nutrient availability increased[109]. During the artificial restoration of alpine mining areas in the Qilian Mountains, Gemmatimonadota remained a dominant bacterial community, but its distribution and structure were significantly impacted by the degree of vegetation restoration and subsequent increases in soil water content, total N, and total phosphorus[110]. Overall, while Gemmatimonadota are well-adapted to barren, hyperarid, or nutrient-poor conditions, they tend to be outcompeted and decrease in relative abundance when vegetation increases and improves soil fertility in high-altitude ecosystems.

Microbial abundance increases with limited diversity gain

Despite the clear increase in microbial abundance with vegetation extent, taxonomic alpha diversity plateaued at intermediate vegetation cover. In contrast, a study on Swiss alpine soils found higher diversity at neutral pH than acidic pH, indicating that neutral soils with lower vegetation density harbor more diverse bacterial communities[24]. Interestingly, they also found that diversity dropped at intermediate altitude (~ 1800 m a.s.l.) but increased again at higher altitudes (~ 2800 m a.s.l.), which might indicate a disconnection between diversity and vegetation cover[24]. A study on Tibetan Plateau found irregular shifts in alpha diversity along a vegetation biomass gradient, while bacterial and fungal beta diversity increased[95]. Desert soils, that are comparable to our barren soil sites in soil properties and microbial communities, exhibited a significant increase in alpha diversity across a vegetation succession gradient[100, 111].

However, our observation of non-linear relationship between microbial diversity and vegetation cover could due to a negative effect of specialist speciation on alpha diversity through environmental filtering[112]. In that case, early vegetation succession would initially promote diversity due to input of new resources but eventually stops because of high selection pressure at denser vegetation cover.

Although flow cytometry has some inherent methodological limitations in estimating in situ cell numbers[55], we do detect clear differences between barren and vegetated soils in orders of magnitudes. We believe that this highlights our gradient in cell numbers as an appropriate indication for increased microbial abundance in vegetated soils.

C cycling under alpine greening

In vegetated alpine permafrost-affected soils, starch, hemicellulose, and cellulose can provide substrates for carbohydrate active enzymes (CAZymes)[87, 89, 113]. The increased abundance of CAZymes in our more vegetated soils supports this interpretation. CAZymes (including glycoside hydrolases, glycosyltransferases, carbohydrate esterases, polysaccharide lyases, and auxiliary activity enzymes) mediate plant polymer degradation[39–41]. Their enrichment in vegetated soils suggests intensified C degradation potential under alpine greening.

This finding aligns with reports of increased CAZyme expression and microbial respiration following root exudate additions in permafrost soils[38] and with positive priming effects described in Arctic systems[114, 115]. However, unlike Arctic peatlands where thaw frequently enhances anaerobic decomposition and CH_4 production[116], the relatively dry and aerated alpine soils studied here appear to favor heterotrophic CO_2 production and CH_4 oxidation.

Strong taxonomy–function coupling challenges the redundancy hypothesis

Contrary to what we hypothesized, functional profiles closely mirrored taxonomic patterns, indicating limited functional redundancy across sites. Communities that were taxonomically distinct also differed in KEGG Ortholog (KO) based functional composition. This strong concordance suggests that shifts in community composition under greening are likely to translate directly into altered metabolic functional potential, with reduced functional redundancy[42, 96].

C cycling gene abundances increased significantly in vegetated soils, whereas their functional diversity plateaued, similarly to taxonomic diversity. This pattern implies an increase of specific metabolic pathways rather than expansion of functional breadth.

Barren soils exhibited comparatively low gene abundances involved in C degradation, consistent with lower CO_2 fluxes in microcosm incubations. In the most vegetated soil, higher CAZyme gene abundance corresponded with elevated CO_2 emissions, supporting a mechanistic link between vegetation-driven substrate input, microbial functional potential, and C mineralization[42, 96].

Differential environmental controls on C, N, and S cycling

C cycling genes were most strongly associated with vegetation extent, but also N and S cycling gene potentials were influenced by vegetation cover more than soil temperature and soil moisture. Vegetation directly supplies organic substrates that stimulate heterotrophic respiration and CAZyme production[42]. In contrast, N and S transformations—such as nitrification, denitrification, and sulfur oxidation—are often found to be more sensitive to redox conditions, soil water content, and temperature[90, 117].

Our microcosm data indicate that vegetated alpine soils function as modest CO_2 sources and potential CH_4 sinks under oxic conditions in summer. Methane has a substantially higher global warming potential than CO_2[118, 119], and its sole ecological sink are soils[119]. Methane oxidation is mediated by methanotrophic bacteria, including atmospheric methane-oxidizing bacteria capable of consuming CH_4

at low concentrations[120, 121]. The predominance of well-drained alpine soils likely suppresses methanogenesis while promoting aerobic CH_4 oxidation[120, 121].

Implications for alpine greening and permafrost feedbacks

Our findings suggest that the ongoing alpine greening in the European Alps[30] will restructure microbial communities towards more abundant, specialist-dominated assemblages with enhanced C processing capacity[96],[91]. This shift may increase CO_2 emissions from alpine permafrost-affected soils, reinforcing climate–carbon feedbacks[122].

At the same time, the relatively thick active layer characteristic of alpine permafrost[123] and the limited vertical differentiation observed within the upper 15 cm indicate that microbial community changes may occur primarily in surface soils. Deeper sampling is required to assess potential transitions toward anaerobic metabolisms and methanogenesis in lower horizons[124].

Compared to Arctic lowland systems, alpine soils exhibit lower C stocks, greater geological heterogeneity, and stronger microclimatic variability[3, 10, 17, 20]. These differences may constrain large-scale CO_2 emissions but enhance sensitivity to vegetation-mediated shifts in heterotrophic respiration[91, 96]. Thus, extrapolation from Arctic permafrost systems to alpine environments remains inappropriate without region-specific data.

Future research could integrate seasonal and diurnal variability, experimental warming, and vegetation manipulation studies to disentangle causal mechanisms. Linking metagenomic potential with transcriptomic activity and *in situ* flux measurements will be critical to refine projections of greenhouse gas dynamics under continued alpine greening.

Conclusion

Alpine greening in European permafrost-affected soils is associated with vegetation-mediated shifts in pH and C:N ratio that restructure microbial communities from generalist-dominated, low-abundance assemblages in barren soils to more abundant, specialist-rich communities in vegetated soils. Functional genetic potential, particularly for CAZymes and trace gas cycling pathways, increases in parallel with vegetation cover and closely tracks taxonomic composition, indicating limited redundancy.

This study provides a more thorough understanding of microbial communities in European alpine permafrost-affected soils and their functional genetic potential. Our findings highlight the need for a better understanding of these vulnerable, rapidly changing environments and their responses to future challenges such as warming and upward vegetation shifts.

Our results suggest that vegetation expansion under climate warming will amplify microbial C processing and potentially CO_2 emissions. Alpine permafrost ecosystems, though spatially fragmented

and comparatively low in C stocks, may therefore contribute non-negligibly to regional climate feedback as greening progresses.

Abbreviations

Adj. p
adjusted *p*–value
ANI
average nucleotide identity
BH
Benjamini–Hochberg correction
bp
base pairs
C
carbon
C:N ratio
carbon–to–nitrogen ratio
CAZy
Carbohydrate–Active enZYmes database
CAZyme
carbohydrate–active enzyme
CH_4
methane
CO
carbon monoxide
CO_2
carbon dioxide
contig
contiguous assembled DNA sequence
DNA
deoxyribonucleic acid
FDR
false discovery rate
GAM
generalized additive model
GH
glycoside hydrolases (a CAZyme class)
GHG
greenhouse gases
GT

glycosyltransferases (a CAZyme class)

H_2

hydrogen

KEGG

Kyoto Encyclopedia of Genes and Genomes

KO

KEGG ortholog

LFC

log fold change

MAGs

metagenome–assembled genomes

m a.s.l.

meters above sea level

N

nitrogen

NMDS

non–metric multidimensional scaling

PCA

principal component analysis

S

sulfur

SWC

soil water content

TC

total carbon

TH

total hydrogen

TN

total nitrogen

TOC

total organic carbon

UV

ultraviolet radiation

16S rRNA

16S ribosomal RNA gene

Declarations

Ethics approval and consent to participate

Not applicable.

Consent for publication

Not applicable.

Competing interests

The authors declare that they have no competing interests.

Funding

We thank the Swiss National Science Foundation (SNSF) for funding (project number IC00I0-231634). **M.B.** acknowledges funding from SNSF NCCR Microbiomes (grant number 225148). **A.S.** acknowledges funding from the Research Council of Norway (FRIPRO project SHRINK, 344999).

Author Contribution

L.A.: conducted laboratory work, bioinformatic processing, data analysis and interpretation, generation of figures, writing and revising manuscript; M.B.: bioinformatic processing, aided in analysis and interpretation of data, revising manuscript; E.V.O.: contributed to conception and design of the study, organized and led the sample collection, optimization of extraction protocols, revising manuscript. G.P.B.: assisted in metagenomics library preparations; A.K.: assisted in sample collection; G.M.: assisted in sample collection; R.C.: optimization of extraction protocols, advice on flow cytometry, revising manuscript; B.F.: contributed to conception and design of the study, revising manuscript; A.S.: interpretation of data, revising manuscript; I.A.: contributed to conception and design of the study, interpretation of data, revising manuscript.

Acknowledgement

We wish to thank our colleague at EPFL, Minju Lee, for laboratory support, and our collaborator at UNIL, Dr. Brahimsamba Bomou, for support with soil CHN analysis. Finally, we wish to acknowledge the online community at Stack-overflow and the open AI ChatGTP, both which have been valuable resources for the bioinformatic work of this study.

Data Availability

The raw sequencing reads for metagenomes generated in this study are publicly available in ENA under the project accession PRJEB109934 (https://www.ebi.ac.uk/ena/browser/view/PRJEB109934) and for 16S rRNA gene amplicons under the project accession PRJEB111633 (https://www.ebi.ac.uk/ena/browser/view/PRJEB111633). Processed datasets and associated

metadata are provided in Zenodo (https://doi.org/10.5281/zenodo.19549183). All scripts used for sequence processing, statistical analyses, and figure generation are available in a Github repository (https://github.com/leeen31/European_high_altitude_soil_microbiome_study). Additionally, the soil metadata are provided in Supplementary file S1-2. More details on statistical tests and analysis on the microbial community composition data can be found in Supplementary file S10-14, on the functional gene abundances in Supplementary file S19-25 and on gas exchange rates in Supplementary file S24-25.

References

1. Schuur Ea, McGuire G, Schädel AD, Grosse C, Harden G, Hayes JW. Climate change and the permafrost carbon feedback. Nat Nat Publishing Group. 2015;520:171–9. https://doi.org/10.1038/nature14338.
2. Altshuler I, Goordial J, Whyte L. Microbial Life in Permafrost. Psychrophiles Biodivers Biotechnol Second Ed. 2017. pp. 153–79. https://doi.org/10.1007/978-3-319-57057-0_8
3. Donhauser J, Frey B. Alpine soil microbial ecology in a changing world. FEMS Microbiol Ecol. 2018;94:fiy099. https://doi.org/10.1093/femsec/fiy099.
4. Weintraub M. Biological Phosphorus Cycling in Arctic and Alpine Soils. 2011. pp. 295–316. https://doi.org/10.1007/978-3-642-15271-9_12
5. Fuchs M, Kuhry P, Hugelius G. Low below-ground organic carbon storage in a subarctic Alpine permafrost environment. Cryosphere. 2015;9:427–38. https://doi.org/10.5194/tc-9-427-2015.
6. Auer I, Böhm R, Jurkovic A, Lipa W, Orlik A, Potzmann R, et al. HISTALP—historical instrumental climatological surface time series of the Greater Alpine Region. Int J Climatol. 2007;27:17–46. https://doi.org/10.1002/joc.1377.
7. Beniston M, Farinotti D, Stoffel M, Andreassen LM, Coppola E, Eckert N, et al. The European mountain cryosphere: a review of its current state, trends, and future challenges. Cryosphere Copernicus GmbH. 2018;12:759–94. https://doi.org/10.5194/tc-12-759-2018.
8. Gobiet A, Kotlarski S, Beniston M, Heinrich G, Rajczak J, Stoffel M. 21st century climate change in the European Alps—A review. Sci Total Environ. 2014;493:1138–51. https://doi.org/10.1016/j.scitotenv.2013.07.050.
9. Rumpf SB, Gravey M, Brönnimann O, Luoto M, Cianfrani C, Mariethoz G, et al. From white to green: Snow cover loss and increased vegetation productivity in the European Alps. Sci Am Association Advancement Sci. 2022;376:1119–22. https://doi.org/10.1126/science.abn6697.
10. Pfiffner OA. Geology of the Alps. Wiley; 2014.
11. Cruz Nunes F, Delunel R, Schlunegger F, Akçar N, Kubik PW. Bedrock bedding, landsliding and erosional budgets in the Central European Alps. Terra Nova. 2015;27:370–8. https://doi.org/10.1111/ter.12169.
12. Dürst Stucki M, Schlunegger F. Identification of erosional mechanisms during past glaciations based on a bedrock surface model of the central European Alps. Earth Planet Sci Lett. 2013;384:57–70.

https://doi.org/10.1016/j.epsl.2013.10.009.
13. Dal Piaz G, Bistacchi A, Massironi M. Geological outline of the Alps. Episodes. 2003;26:175–80. https://doi.org/10.18814/epiiugs/2003/v26i3/004.
14. Ivy-Ochs S. Glacier variations in the European Alps at the end of the last glaciation. Cuad Investig Geográfica. 2015;41:295. https://doi.org/10.18172/cig.2750.
15. Sommer C, Malz P, Seehaus TC, Lippl S, Zemp M, Braun MH. Rapid glacier retreat and downwasting throughout the European Alps in the early 21st century. Nat Commun Nat Publishing Group. 2020;11:3209. https://doi.org/10.1038/s41467-020-16818-0.
16. Diolaiuti G, Maragno D, D'Agata C, Smiraglia C, Bocchiola D. Glacier retreat and climate change: Documenting the last 50 years of Alpine glacier history from area and geometry changes of Dosde Piazzi glaciers (Lombardy Alps, Italy). Prog Phys Geogr. 2011;35:161–82. https://doi.org/10.1177/0309133311399494.
17. Boeckli L, Brenning A, Gruber S, Noetzli J. Permafrost distribution in the European Alps: calculation and evaluation of an index map and summary statistics. Cryosphere Copernicus GmbH. 2012;6:807–20. https://doi.org/10.5194/tc-6-807-2012.
18. Kenner R, Noetzli J, Hoelzle M, Raetzo H, Phillips M. Distinguishing ice-rich and ice-poor permafrost to map ground temperatures and ground ice occurrence in the Swiss Alps. Cryosphere Copernicus GmbH. 2019;13:1925–41. https://doi.org/10.5194/tc-13-1925-2019.
19. Gruber S, Haeberli W. Mountain Permafrost. Permafr Soils. 2009. pp. 33–44. https://doi.org/10.1007/978-3-540-69371-0_3
20. King AJ, Freeman KR, McCormick KF, Lynch RC, Lozupone C, Knight R, et al. Biogeography and habitat modelling of high-alpine bacteria. Nat Commun Nat Publishing Group. 2010;1:53. https://doi.org/10.1038/ncomms1055.
21. Göransson H, Olde Venterink H, Bååth E. Soil bacterial growth and nutrient limitation along a chronosequence from a glacier forefield. Soil Biol Biochem. 2011;43:1333–40. https://doi.org/10.1016/j.soilbio.2011.03.006.
22. CHARLIER RH. The Geographic Distribution of Polar Desert Soils in the Northern Hemisphere. GSA Bull. 1969;80:1985–96. https://doi.org/10.1130/0016-7606.(1969)80%255B1985:TGDOPD%255D2.0.CO;2.
23. Romanovskii NN, Hubberten H-W, Gavrilov AV, Tumskoy VE, Kholodov AL. Permafrost of the east Siberian Arctic shelf and coastal lowlands. Quat Sci Rev. 2004;23:1359–69. https://doi.org/10.1016/j.quascirev.2003.12.014.
24. Yashiro E, Pinto-Figueroa E, Buri A, Spangenberg JE, Adatte T, Niculita-Hirzel H, et al. Local Environmental Factors Drive Divergent Grassland Soil Bacterial Communities in the Western Swiss Alps. Appl Environ Microbiol Am Soc Microbiol. 2016;82:6303–16. https://doi.org/10.1128/AEM.01170-16.
25. Sannino C, Borruso L, Mezzasoma A, Battistel D, Ponti S, Turchetti B, et al. Abiotic factors affecting the bacterial and fungal diversity of permafrost in a rock glacier in the Stelvio Pass (Italian Central

Alps). Appl Soil Ecol. 2021;166:104079. https://doi.org/10.1016/j.apsoil.2021.104079.

26. Perez-Mon C, Qi W, Vikram S, Frossard A, Makhalanyane T, Cowan D, et al. Shotgun metagenomics reveals distinct functional diversity and metabolic capabilities between 12 000-year-old permafrost and active layers on Muot da Barba Peider (Swiss Alps). Microb Genomics. 2021;7:000558. https://doi.org/10.1099/mgen.0.000558.
27. Zhang X, Xu S, Li C, Zhao L, Feng H, Yue G, et al. The soil carbon/nitrogen ratio and moisture affect microbial community structures in alkaline permafrost-affected soils with different vegetation types on the Tibetan plateau. Res Microbiol. 2014;165:128–39. https://doi.org/10.1016/j.resmic.2014.01.002.
28. Malard LA, Anwar MZ, Jacobsen CS, Pearce DA. Biogeographical patterns in soil bacterial communities across the Arctic region. FEMS Microbiol Ecol. 2019;95:fiz128. https://doi.org/10.1093/femsec/fiz128.
29. Choler P, Bayle A, Carlson BZ, Randin C, Filippa G, Cremonese E. The tempo of greening in the European Alps: Spatial variations on a common theme. Glob Change Biol. 2021;27:5614–28. https://doi.org/10.1111/gcb.15820.
30. Vanneste T, Pauli H, Dullinger S, Graae B, Verheyen K, Frenne P et al. Widespread shrubification on European mountain summits. 2025. https://doi.org/10.21203/rs.3.rs-7431847/v1
31. Hagedorn F, Gavazov K, Alexander JM. Above- and belowground linkages shape responses of mountain vegetation to climate change. Sci Am Association Advancement Sci. 2019;365:1119–23. https://doi.org/10.1126/science.aax4737.
32. Frost GV, Bhatt US, Macander MJ, Berner LT, Walker DA, Raynolds MK, et al. The changing face of the Arctic: four decades of greening and implications for tundra ecosystems. Front Environ Sci [Internet] Front. 2025. https://doi.org/10.3389/fenvs.2025.1525574. [cited 2025 Dec 17];13.
33. Phoenix GK, Treharne R. Arctic greening and browning: Challenges and a cascade of complexities. Glob Change Biol. 2022;28:3481–3. https://doi.org/10.1111/gcb.16118.
34. Myers-Smith IH, Kerby JT, Phoenix GK, Bjerke JW, Epstein HE, Assmann JJ, et al. Complexity revealed in the greening of the Arctic. Nat Clim Change Nat Publishing Group. 2020;10:106–17. https://doi.org/10.1038/s41558-019-0688-1.
35. Voigt C, Lamprecht RE, Marushchak ME, Lind SE, Novakovskiy A, Aurela M, et al. Warming of subarctic tundra increases emissions of all three important greenhouse gases – carbon dioxide, methane, and nitrous oxide. Glob Change Biol. 2017;23:3121–38. https://doi.org/10.1111/gcb.13563.
36. Feng M, Varliero G, Perez-Mon C, Robinson S, Qi W, Stierli B, et al. Permafrost thawing by soil transplantation alters the functional genetic potential of the alpine permafrost microbiome. Geoderma. 2025;458:117339. https://doi.org/10.1016/j.geoderma.2025.117339.
37. The CAZypedia Consortium. Ten years of CAZypedia: a living encyclopedia of carbohydrate-active enzymes. Glycobiology. 2018;28:3–8. https://doi.org/10.1093/glycob/cwx089.

38. Adamczyk M, Rüthi J, Frey B. Root exudates increase soil respiration and alter microbial community structure in alpine permafrost and active layer soils. Environ Microbiol. 2021;23:2152–68. https://doi.org/10.1111/1462-2920.15383.
39. Ten years of CAZypedia. a living encyclopedia of carbohydrate-active enzymes | Glycobiology | Oxford Academic [Internet]. [cited 2025 Dec 17]. https://academic.oup.com/glycob/article/28/1/3/4430919. Accessed 17 Dec 2025.
40. Cantarel BL, Coutinho PM, Rancurel C, Bernard T, Lombard V, Henrissat B. The Carbohydrate-Active EnZymes database (CAZy): an expert resource for Glycogenomics. Nucleic Acids Res Oxf Acad. 2009;37:D233–8. https://doi.org/10.1093/nar/gkn663.
41. Lombard V, Golaconda Ramulu H, Drula E, Coutinho PM, Henrissat B. The carbohydrate-active enzymes database (CAZy) in 2013. Nucleic Acids Res Oxf Acad. 2014;42:D490–5. https://doi.org/10.1093/nar/gkt1178.
42. D'Alò F, Baldrian P, Odriozola I, Morais D, Větrovský T, Zucconi L, et al. Composition and functioning of the soil microbiome in the highest altitudes of the Italian Alps and potential effects of climate change. FEMS Microbiol Ecol. 2022;98:fiac025. https://doi.org/10.1093/femsec/fiac025.
43. Olivas PC, Oberbauer SF, Tweedie C, Oechel WC, Lin D, Kuchy A. Effects of Fine-Scale Topography on CO2 Flux Components of Alaskan Coastal Plain Tundra: Response to Contrasting Growing Seasons. Arct Antarct Alp Res Taylor Francis. 2011;43:256–66. https://doi.org/10.1657/1938-4246-43.2.256.
44. Mauritz M, Bracho R, Celis G, Hutchings J, Natali SM, Pegoraro E, et al. Nonlinear CO2 flux response to 7 years of experimentally induced permafrost thaw. Glob Change Biol. 2017;23:3646–66. https://doi.org/10.1111/gcb.13661.
45. Rustad L, Campbell J, Marion G, Norby R, Mitchell M, Hartley A, et al. A meta-analysis of the response of soil respiration, net nitrogen mineralization, and aboveground plant growth to experimental ecosystem warming. Oecologia. 2001;126:543–62. https://doi.org/10.1007/s004420000544.
46. Altshuler I, Hamel J, Turney S, Magnuson E, Lévesque R, Greer CW, et al. Species interactions and distinct microbial communities in high Arctic permafrost affected cryosols are associated with the CH4 and CO2 gas fluxes. Environ Microbiol. 2019;21:3711–27. https://doi.org/10.1111/1462-2920.14715.
47. Lau MCY, Stackhouse BT, Layton AC, Chauhan A, Vishnivetskaya TA, Chourey K, et al. An active atmospheric methane sink in high Arctic mineral cryosols. ISME J Nat Publishing Group. 2015;9:1880–91. https://doi.org/10.1038/ismej.2015.13.
48. Bosch A, Schmidt K, He J-S, Doerfer C, Scholten T. Potential CO2 emissions from defrosting permafrost soils of the Qinghai-Tibet Plateau under different scenarios of climate change in 2050 and 2070. CATENA. 2017;149:221–31. https://doi.org/10.1016/j.catena.2016.08.035.
49. Cheng F, Garzione C, Li X, Salzmann U, Schwarz F, Haywood AM, et al. Alpine permafrost could account for a quarter of thawed carbon based on Plio-Pleistocene paleoclimate analogue. Nat Commun Nat Publishing Group. 2022;13:1329. https://doi.org/10.1038/s41467-022-29011-2.

50. Wei D, Qi Y, Ma Y, Wang X, Ma W, Gao T et al. Plant uptake of CO2 outpaces losses from permafrost and plant respiration on the Tibetan Plateau. Proc Natl Acad Sci. Proceedings of the National Academy of Sciences; 2021;118:e2015283118. https://doi.org/10.1073/pnas.2015283118
51. Lithological map of. Switzerland 1:500000 [Internet]. geocat.ch. [cited 2024 Nov 21]. https://www.geocat.ch/geonetwork/srv/api/records/435522fb-599e-41c0-a7c0-49d922ea6acf. Accessed 21 Nov 2024.
52. Frehner M, Schwitter R, Brang P, Matter C, Dingwall AS. Sustainability and success monitoring in protection forests.
53. Patrignani A, Ochsner TE, Canopeo. A Powerful New Tool for Measuring Fractional Green Canopy Cover. Agron J. 2015;107:2312–20. https://doi.org/10.2134/agronj15.0150.
54. Górniak D, Marszałek H, Kwaśniak-Kominek M, Rzepa G, Manecki M. Soil formation and initial microbiological activity on a foreland of an Arctic glacier (SW Svalbard). Appl Soil Ecol. 2017;114:34–44. https://doi.org/10.1016/j.apsoil.2017.02.017.
55. Frossard A, Hammes F, Gessner MO. Flow Cytometric Assessment of Bacterial Abundance in Soils, Sediments and Sludge. Front Microbiol [Internet]. Frontiers; 2016 [cited 2025 Dec 12];7. https://doi.org/10.3389/fmicb.2016.00903
56. Krueger F, James F, Ewels P, Afyounian E, Weinstein M, Schuster-Boeckler B et al. TrimGalore [Internet]. Github repository; 2021 [cited 2025 Dec 15]. https://doi.org/10.5281/zenodo.7598955
57. Li D, Liu C-M, Luo R, Sadakane K, Lam T-W. MEGAHIT: an ultra-fast single-node solution for large and complex metagenomics assembly via succinct de Bruijn graph. Bioinformatics. 2015;31:1674–6. https://doi.org/10.1093/bioinformatics/btv033.
58. Mikheenko A, Saveliev V, Gurevich A. MetaQUAST: evaluation of metagenome assemblies. Bioinformatics. 2016;32:1088–90. https://doi.org/10.1093/bioinformatics/btv697.
59. Shen W, Le S, Li Y, Hu F, SeqKit:. A Cross-Platform and Ultrafast Toolkit for FASTA/Q File Manipulation. PLOS ONE Public Libr Sci. 2016;11:e0163962. https://doi.org/10.1371/journal.pone.0163962.
60. CoverM. Read coverage calculator for metagenomics [Internet]. [cited 2024 Nov 7]. https://zenodo.org/records/10531254. Accessed 7 Nov 2024.
61. Li H. Minimap2: pairwise alignment for nucleotide sequences. Bioinformatics. 2018;34:3094–100. https://doi.org/10.1093/bioinformatics/bty191.
62. Kang DD, Li F, Kirton E, Thomas A, Egan R, An H, et al. MetaBAT 2: an adaptive binning algorithm for robust and efficient genome reconstruction from metagenome assemblies. PeerJ. 2019;7:e7359. https://doi.org/10.7717/peerj.7359.
63. Wu Y-W, Simmons BA, Singer SW. MaxBin 2.0: an automated binning algorithm to recover genomes from multiple metagenomic datasets. Bioinforma Oxf Engl. 2016;32:605–7. https://doi.org/10.1093/bioinformatics/btv638.
64. Newell R. rosella [Internet]. 2024 [cited 2025 Dec 15]. https://github.com/rhysnewell/rosella. Accessed 15 Dec 2025.

65. Mainguy J, Hoede C. Binette: a fast and accurate bin refinement tool to construct high quality Metagenome Assembled Genomes. 2024. https://doi.org/10.1101/2024.04.20.585171
66. Chklovski A, Parks DH, Woodcroft BJ, Tyson GW. CheckM2: a rapid, scalable and accurate tool for assessing microbial genome quality using machine learning. Nat Methods Nat Publishing Group. 2023;20:1203–12. https://doi.org/10.1038/s41592-023-01940-w.
67. Westgate M, Kellie D, Stevenson M, Newman P. galah: Biodiversity Data from the GBIF Node Network [Internet]. 2025 [cited 2025 Dec 15]. https://CRAN.R-project.org/package=galah. Accessed 15 Dec 2025.
68. Chaumeil P-A, Mussig AJ, Hugenholtz P, Parks DH. GTDB-Tk: a toolkit to classify genomes with the Genome Taxonomy Database. Bioinforma Oxf Engl. 2019;36:1925–7. https://doi.org/10.1093/bioinformatics/btz848.
69. Wood DE, Lu J, Langmead B. Improved metagenomic analysis with Kraken 2. Genome Biol. 2019;20:257. https://doi.org/10.1186/s13059-019-1891-0.
70. Cantalapiedra CP, Hernández-Plaza A, Letunic I, Bork P, Huerta-Cepas J. eggNOG-mapper v2: Functional Annotation, Orthology Assignments, and Domain Prediction at the Metagenomic Scale. Mol Biol Evol. 2021;38:5825–9. https://doi.org/10.1093/molbev/msab293.
71. Steinegger M, Söding J. MMseqs2 enables sensitive protein sequence searching for the analysis of massive data sets. Nat Biotechnol Nat Publishing Group. 2017;35:1026–8. https://doi.org/10.1038/nbt.3988.
72. Leung PM, Greening C. Greening lab metabolic marker gene databases. 2020. https://doi.org/10.26180/c.5230745
73. Karlicki M, Antonowicz S, Karnkowska A. Tiara: deep learning-based classification system for eukaryotic sequences. Bioinformatics. 2022;38:344–50. https://doi.org/10.1093/bioinformatics/btab672.
74. R Core Team. R: a language and environment for statistical computing [Internet]. Vienna, Austria: R Foundation for Statistical Computing; 2025. https://www.R-project.org/.
75. Posit team. RStudio: Integrated development environment for R [Internet]. Boston, MA: Posit Software, PBC; 2025. http://www.posit.co/.
76. Wickham H. ggplot2: Elegant graphics for data analysis [Internet]. Springer-Verlag New York; 2016. https://ggplot2.tidyverse.org
77. William Revelle. psych: Procedures for psychological, psychometric, and personality research [Internet]. Evanston, Illinois: Northwestern University; 2025. https://CRAN.R-project.org/package=psych.
78. Peterson RA. Finding optimal normalizing transformations via bestNormalize. R J. 2021;13:310–29. https://doi.org/10.32614/RJ-2021-041.
79. Oksanen J, Simpson GL, Blanchet FG, Kindt R, Legendre P, Minchin PR et al. vegan: Community ecology package [Internet]. 2025. https://vegandevs.github.io/vegan/

80. Lahti L, Shetty S. microbiome R package. Bioconductor; 2017. https://doi.org/10.18129/B9.bioc.microbiome
81. Lin H, Peddada SD. Multigroup analysis of compositions of microbiomes with covariate adjustments and repeated measures. Nat Methods. 2024;21:83–91.
82. Luo Z, Liu J, Zhao P, Jia T, Li C, Chai B. Biogeographic Patterns and Assembly Mechanisms of Bacterial Communities Differ Between Habitat Generalists and Specialists Across Elevational Gradients. Front Microbiol [Internet]. Frontiers; 2019 [cited 2026 Mar 25];10. https://doi.org/10.3389/fmicb.2019.00169
83. Pandit SN, Kolasa J, Cottenie K. Contrasts between habitat generalists and specialists: an empirical extension to the basic metacommunity framework. Ecology. 2009;90:2253–62. https://doi.org/10.1890/08-0851.1.
84. LEVINS R. Evolution in Changing Environments [Internet]. Princeton University Press; 1968 [cited 2026 Feb 26]. https://doi.org/10.2307/j.ctvx5wbbh
85. Wood SN. Fast stable restricted maximum likelihood and marginal likelihood estimation of semiparametric generalized linear models. J R Stat Soc B. 2011;73:3–36. https://doi.org/10.1111/j.1467-9868.2010.00749.x.
86. Mitchell RJ, Hester AJ, Campbell CD, Chapman SJ, Cameron CM, Hewison RL, et al. Is vegetation composition or soil chemistry the best predictor of the soil microbial community? Plant Soil. 2010;333:417–30. https://doi.org/10.1007/s11104-010-0357-7.
87. Perez-Mon C, Stierli B, Plötze M, Frey B. Fast and persistent responses of alpine permafrost microbial communities to in situ warming. Sci Total Environ. 2022;807:150720. https://doi.org/10.1016/j.scitotenv.2021.150720.
88. Frey B, Rime T, Phillips M, Stierli B, Hajdas I, Widmer F, et al. Microbial diversity in European alpine permafrost and active layers. FEMS Microbiol Ecol. 2016;92:fiw018. https://doi.org/10.1093/femsec/fiw018.
89. Feng M, Varliero G, Qi W, Stierli B, Edwards A, Robinson S, et al. Microbial dynamics in soils of the Damma glacier forefield show succession in the functional genetic potential. Environ Microbiol. 2023;25:3116–38. https://doi.org/10.1111/1462-2920.16497.
90. Chen Y-L, Ding J-Z, Peng Y-F, Li F, Yang G-B, Liu L, et al. Patterns and drivers of soil microbial communities in Tibetan alpine and global terrestrial ecosystems. J Biogeogr. 2016;43:2027–39. https://doi.org/10.1111/jbi.12806.
91. Chen L, Liang J, Qin S, Liu L, Fang K, Xu Y, et al. Determinants of carbon release from the active layer and permafrost deposits on the Tibetan Plateau. Nat Commun. 2016;7:13046. https://doi.org/10.1038/ncomms13046.
92. Adamczyk M, Hagedorn F, Wipf S, Donhauser J, Vittoz P, Rixen C, et al. The Soil Microbiome of GLORIA Mountain Summits in the Swiss Alps. Front Microbiol [Internet] Front. 2019. https://doi.org/10.3389/fmicb.2019.01080. [cited 2025 Oct 14];10.

93. Choe Y-H, Kim M, Woo J, Lee MJ, Lee JI, Lee EJ, et al. Comparing rock-inhabiting microbial communities in different rock types from a high arctic polar desert. FEMS Microbiol Ecol. 2018;94:fiy070. https://doi.org/10.1093/femsec/fiy070.
94. Chen Y-L, Chen L-Y, Peng Y-F, Ding J-Z, Li F, Yang G-B, et al. Linking microbial C:N:P stoichiometry to microbial community and abiotic factors along a 3500-km grassland transect on the Tibetan Plateau. Glob Ecol Biogeogr. 2016;25:1416–27. https://doi.org/10.1111/geb.12500.
95. Wu M-H, Xue K, Wei P-J, Jia Y-L, Zhang Y, Chen S-Y. Soil microbial distribution and assembly are related to vegetation biomass in the alpine permafrost regions of the Qinghai-Tibet Plateau. Sci Total Environ. 2022;834:155259. https://doi.org/10.1016/j.scitotenv.2022.155259.
96. Ma S, Zhu W, Wang W, Li X, Sheng Z. Microbial assemblies with distinct trophic strategies drive changes in soil microbial carbon use efficiency along vegetation primary succession in a glacier retreat area of the southeastern Tibetan Plateau. Sci Total Environ. 2023;867:161587. https://doi.org/10.1016/j.scitotenv.2023.161587.
97. Rime T, Hartmann M, Brunner I, Widmer F, Zeyer J, Frey B. Vertical distribution of the soil microbiota along a successional gradient in a glacier forefield. Mol Ecol. 2015;24:1091–108. https://doi.org/10.1111/mec.13051.
98. Székely AJ, Langenheder S. The importance of species sorting differs between habitat generalists and specialists in bacterial communities. FEMS Microbiol Ecol. 2014;87:102–12. https://doi.org/10.1111/1574-6941.12195.
99. Bell TH, Bell T. Many roads to bacterial generalism. FEMS Microbiol Ecol. 2021;97:fiaa240. https://doi.org/10.1093/femsec/fiaa240.
100. Dong R, Wang X, Wang Y, Ma Y, Yang S, Zhang L, et al. Differences in soil microbial communities with successional stage depend on vegetation coverage and soil substrates in alpine desert shrublands. Plant Soil. 2023;485:549–68. https://doi.org/10.1007/s11104-022-05849-9.
101. Bartholomäus A, Genderjahn S, Mangelsdorf K, Schneider B, Zamorano P, Kounaves SP, et al. Inside the Atacama Desert: uncovering the living microbiome of an extreme environment. Appl Environ Microbiol Am Soc Microbiol. 2024;90:e01443–24. https://doi.org/10.1128/aem.01443-24.
102. Schulze-Makuch D, Lipus D, Arens FL, Baqué M, Bornemann TLV, de Vera J-P et al. Microbial Hotspots in Lithic Microhabitats Inferred from DNA Fractionation and Metagenomics in the Atacama Desert. Microorganisms [Internet]. publisher; 2021 [cited 2026 Mar 3];9. https://doi.org/10.3390/microorganisms9051038
103. Hernandez DJ, Kiesewetter KN, Almeida BK, Revillini D, Afkhami ME. Multidimensional specialization and generalization are pervasive in soil prokaryotes. Nat Ecol Evol Nat Publishing Group. 2023;7:1408–18. https://doi.org/10.1038/s41559-023-02149-y.
104. Egerton FN. History of Ecological Sciences, Part 54: Succession, Community, and Continuum. Bull Ecol Soc Am. 2015;96:426–74. https://doi.org/10.1890/0012-9623-96.3.426.
105. Meiners SJ, Cadotte MW, Fridley JD, Pickett STA, Walker LR. Is successional research nearing its climax? New approaches for understanding dynamic communities. Funct Ecol. 2015;29:154–64.

https://doi.org/10.1111/1365-2435.12391.

106. Deonalli D, Sharma R, Jangid K. Microbial Community Dynamics During Soil Ecosystem Development. In: Kalia VC, Shouche Y, Purohit HJ, Rahi P, editors. Min Microb Wealth MetaGenomics [Internet]. Singapore: Springer; 2017 [cited 2026 Mar 3]. pp. 57–82. https://doi.org/10.1007/978-981-10-5708-3_4
107. Xie L, Ma Y, Wang Y, Ma Y, Liu Y. Changes of soil bacterial community composition and functional groups in different altitude gradients of Potentilla fruticosa shrub in eastern Qinghai-Tibet Plateau. Front Plant Sci [Internet]. Frontiers; 2025 [cited 2026 Mar 5];16. https://doi.org/10.3389/fpls.2025.1539945
108. Kumar M, van Elsas JD, Nissinen R. Strong Regionality and Dominance of Anaerobic Bacterial Taxa Characterize Diazotrophic Bacterial Communities of the Arcto-Alpine Plant Species Oxyria digyna and Saxifraga oppositifolia. Front Microbiol [Internet] Front. 2017. https://doi.org/10.3389/fmicb.2017.01972. [cited 2026 Mar 5];8.
109. Li P, Fu W, Bai Y, Zhou D, Sun S, Guo Q, et al. Fungal communities dominate accumulation of microbial necromass carbon after 11-year revegetation in a semi-arid desert mining area. J Environ Manage. 2026;398:128429. https://doi.org/10.1016/j.jenvman.2025.128429.
110. Yang X, Feng Q, Zhu M, Zhang J, Yang L, Li R. The Impact of Artificial Restoration of Alpine Grasslands in the Qilian Mountains on Vegetation, Soil Bacteria, and Soil Fungal Community Diversity. Microorganisms [Internet]. Multidisciplinary Digital Publishing Institute; 2024. [cited 2026 Mar 5];12. https://doi.org/10.3390/microorganisms12050854.
111. Yu J, Yin Q, Niu J, Yan Z, Wang H, Wang Y, et al. Consistent effects of vegetation patch type on soil microbial communities across three successional stages in a desert ecosystem. Land Degrad Dev. 2022;33:1552–63. https://doi.org/10.1002/ldr.4194.
112. Mayfield MM, Levine JM. Opposing effects of competitive exclusion on the phylogenetic structure of communities. Ecol Lett. 2010;13:1085–93. https://doi.org/10.1111/j.1461-0248.2010.01509.x.
113. Donhauser J, Qi W, Bergk-Pinto B, Frey B. High temperatures enhance the microbial genetic potential to recycle C and N from necromass in high-mountain soils. Glob Change Biol. 2021;27:1365–86. https://doi.org/10.1111/gcb.15492.
114. Cuartero J, Perez-Mon C, Qi W, Stierli B, Frey B, Varliero G. Increased carbon inputs alter soil microbial genetic potential for biogeochemical cycling in Arctic ecosystems. Commun Earth Environ Nat Publishing Group. 2025;6:807. https://doi.org/10.1038/s43247-025-02768-2.
115. Adamczyk M, Perez-Mon C, Gunz S, Frey B. Strong shifts in microbial community structure are associated with increased litter input rather than temperature in High Arctic soils. Soil Biol Biochem. 2020;151:108054. https://doi.org/10.1016/j.soilbio.2020.108054.
116. Li Y, Xue Y, Roy Chowdhury T, Graham DE, Tringe SG, Jansson JK, et al. Genomic insights into redox-driven microbial processes for carbon decomposition in thawing Arctic soils and permafrost. mSphere Am Soc Microbiol. 2024;9:e00259–24. https://doi.org/10.1128/msphere.00259-24.

117. Chen Y, Kou D, Li F, Ding J, Yang G, Fang K, et al. Linkage of plant and abiotic properties to the abundance and activity of N-cycling microbial communities in Tibetan permafrost-affected regions. Plant Soil. 2019;434:453–66. https://doi.org/10.1007/s11104-018-3845-9.

118. Mar KA, Unger C, Walderdorff L, Butler T. Beyond CO2 equivalence: The impacts of methane on climate, ecosystems, and health. Environ Sci Policy. 2022;134:127–36. https://doi.org/10.1016/j.envsci.2022.03.027.

119. Masson-Delmotte V, Zhai P, Pirani A, Connors SL, Péan C, Berger S, et al. editors. Climate Change 2021: The Physical Science Basis. Contribution of Working Group I to the Sixth Assessment Report of the Intergovernmental Panel on Climate Change. Cambridge, United Kingdom and New York, NY, USA: Cambridge University Press; 2021. https://doi.org/10.1017/9781009157896.

120. Conrad R. Microbial Ecology of Methanogens and Methanotrophs. Adv Agron [Internet]. Academic Press; 2007 [cited 2024 Nov 7]. pp. 1–63. https://doi.org/10.1016/S0065-2113(07)96005-8

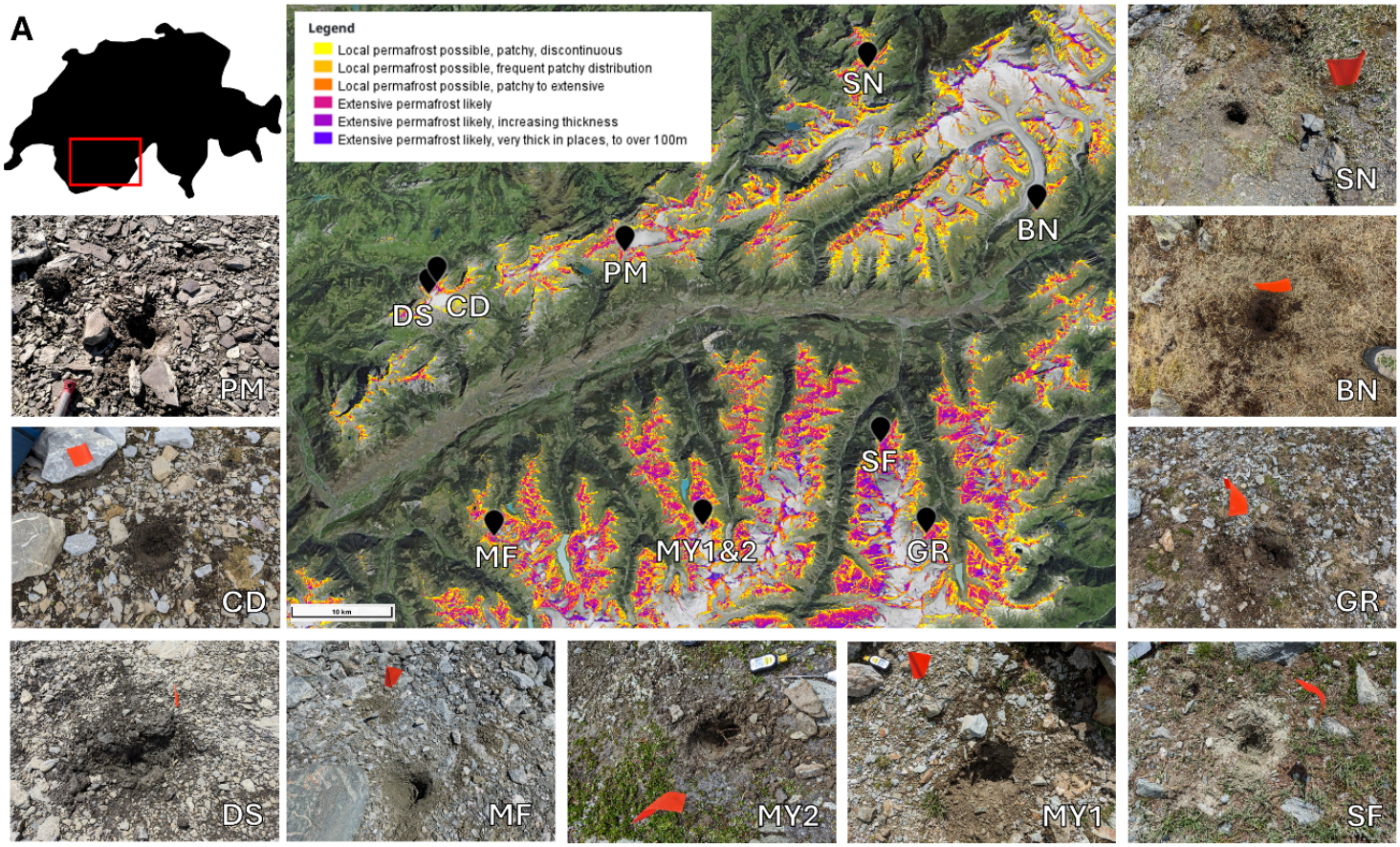
121. Conrad R. Soil microorganisms as controllers of atmospheric trace gases (H2, CO, CH4, OCS, N2O, and NO). Microbiol Rev Am Soc Microbiol. 1996;60:609–40. https://doi.org/10.1128/mr.60.4.609-640.1996.

122. Ding J, Chen L, Zhang B, Liu L, Yang G, Fang K, et al. Linking temperature sensitivity of soil CO2 release to substrate, environmental, and microbial properties across alpine ecosystems. Glob Biogeochem Cycles. 2016;30:1310–23. https://doi.org/10.1002/2015GB005333.

123. Frey B, Rime T, Phillips M, Stierli B, Hajdas I, Widmer F et al. Microbial diversity in European alpine permafrost and active layers. Margesin R, editor. FEMS Microbiol Ecol. 2016;92:fiw018. https://doi.org/10.1093/femsec/fiw018

124. Lyu Z, Shao N, Akinyemi T, Whitman WB, Methanogenesis. Curr Biol Elsevier. 2018;28:R727–32. https://doi.org/10.1016/j.cub.2018.05.021.

Figures



B

	Name	Lithology	Ecoregion	Altitude (m.a.s.l.)	Vegetation (%)	pH	SWC (%)	C:N	TOC (%)	TN (%)
CD	Diablerets	Limestone	Northern pre-alps	2485	2.6	7.0	21.3	63.9	0.96	0.095
SF	Saas Fee	Basic rock	Continental alps	2598	10.9	6.2	6.5	124.4	0.26	0.009
BN	Bettmerhorn	Granites	Continental alps	2625	20.2	3.9	36.8	17.0	6.03	0.360
GR	Grächen	Gneiss	Continental alps	2644	4.4	5.1	12.1	17.8	1.16	0.060
MY2	Moiry 2	Granites	Continental alps	2812	15.0	4.5	17.5	13.8	1.31	0.095
MY1	Moiry 1	Granites	Continental alps	2825	5.3	6.8	12.6	21.7	0.48	0.023
DS	Diablerets Scex Rouge	Limestone	Northern pre-alps	2839	0.5	6.8	15.5	124.9	0.31	0.030
MF	Mont Fort	Mica shists	Continental alps	2885	0.1	6.9	8.8	130.2	0.08	0.001
PM	Plaine Morte	Limestone	Northern pre-alps	2890	0.1	7.1	17.3	66.5	0.06	0.049
SN	Schilthorn	Marly shales	Northern pre-alps	2941	7.9	5.2	6.9	9.3	0.63	0.068

Figure 1

Description and characteristics of ten alpine high-altitude soil sites. A) Location of the sampling sites across the Swiss Alps with close up photographs to illustrate vegetation cover per site. Yellow and purple colors indicate alpine permafrost areas predicted by the Alpine permafrost map index (APMI)[17]. B) Site information and the associated environmental and physicochemical soil properties altitude, vegetation cover, pH, soil water content (SWC), carbon to nitrogen ratio (C:N), total organic carbon (TOC) and total nitrogen (TN). All values are averages per site. Detailed information can be found in Supplementary material Table S1 and Supplementary file S1-2.

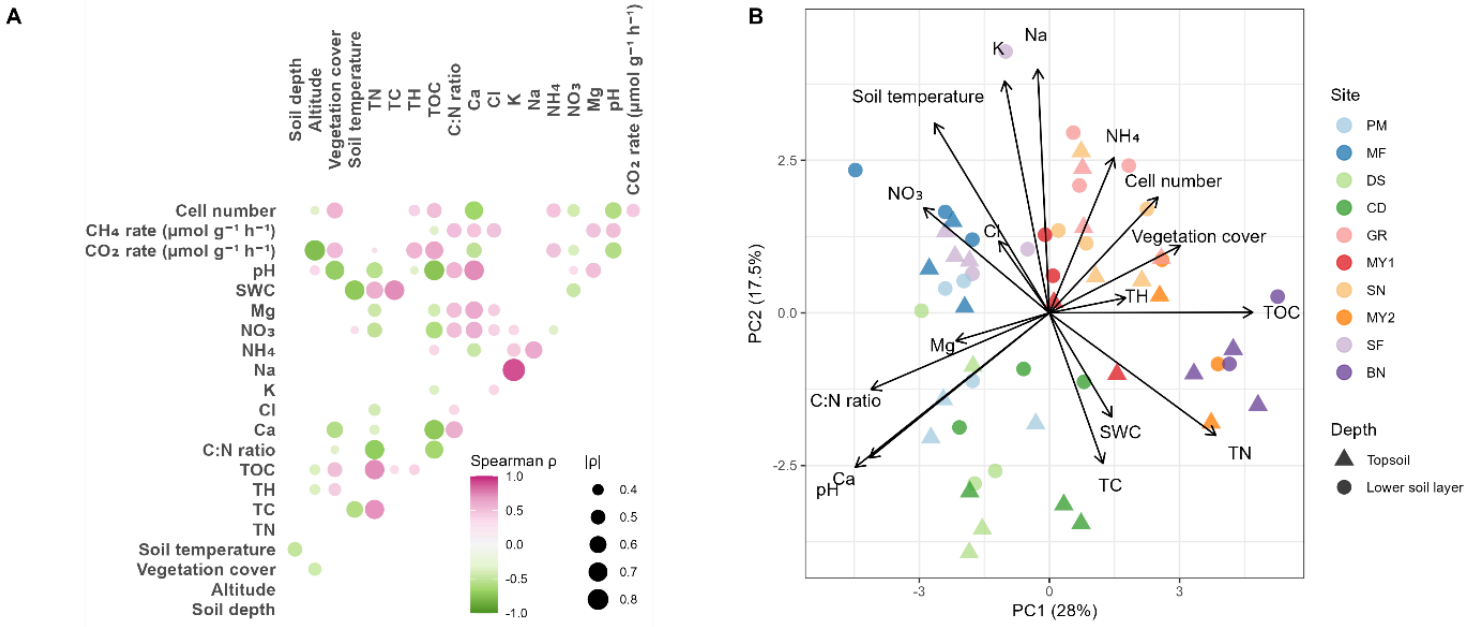


Figure 2

Environmental and soil variables of ten alpine permafrost-affected soils (see Figure 1 for site abbreviations). A) Spearman's correlation of soil physicochemical variables and cell numbers (significance adj. p <0.05). B) Principal Component Analysis (PCA) of soil physicochemical variables across sites and soil depths with environmental drivers (significance adj. p <0.01, see Supplementary file S6-7). Topsoil (0 – 5 cm) and lower soil layer (5 – 15 cm).

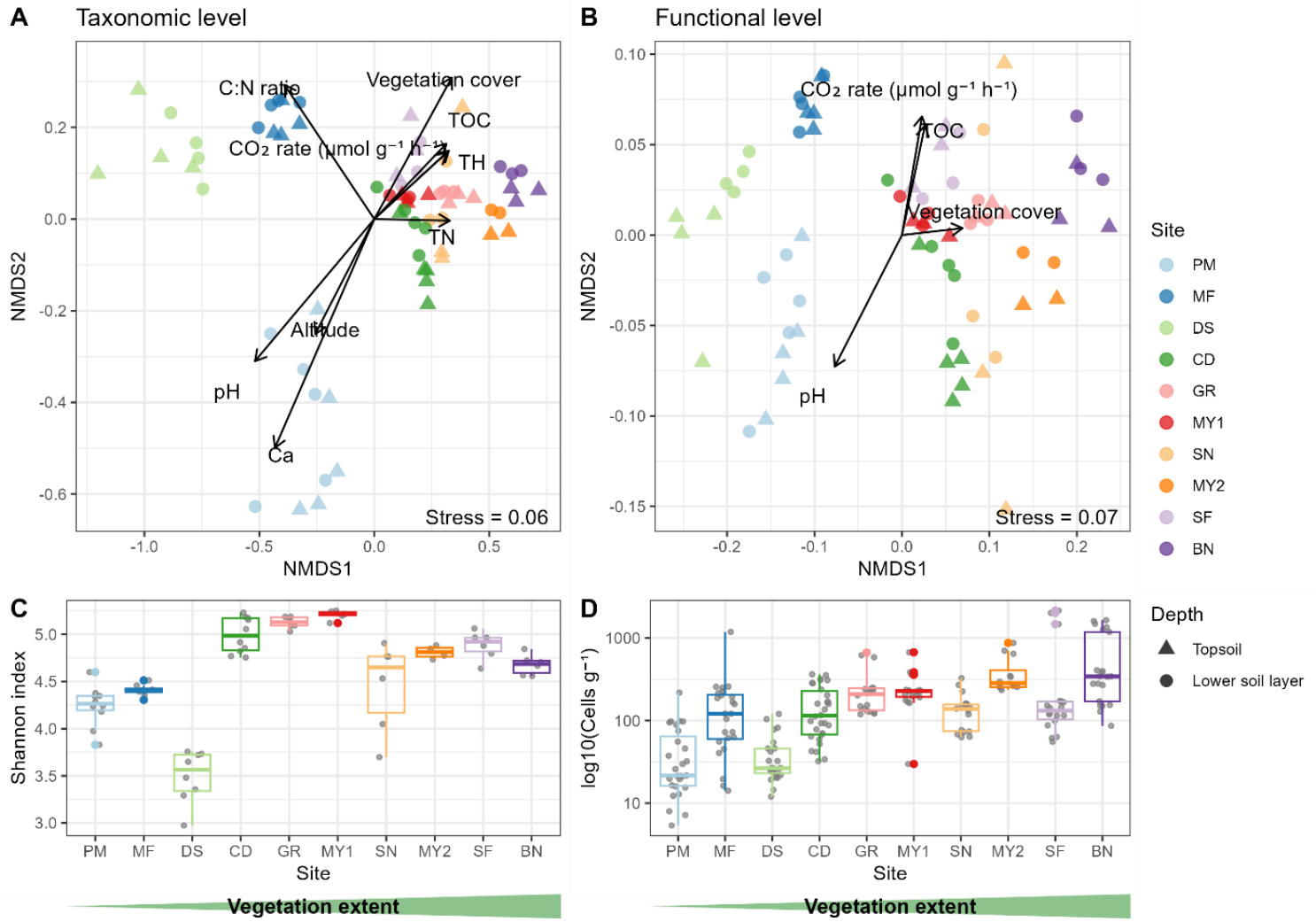


Figure 3

Microbial community characteristics of the ten alpine permafrost-affected soils. Metagenome based non-metric multidimensional scaling (NMDS) of A) taxonomic and B) functional profiles using KEGG Orthology (KO). Only significant drivers ($p < 0.05$) are shown, for details on drivers see Supplementary file S9. Boxplots of C) mean Shannon indices (based on MAGs) and D) cell numbers (log10 transformed) across sites ordered from barren to more vegetated soils. See Supplementary file S10 - S14 for information on statistical tests.

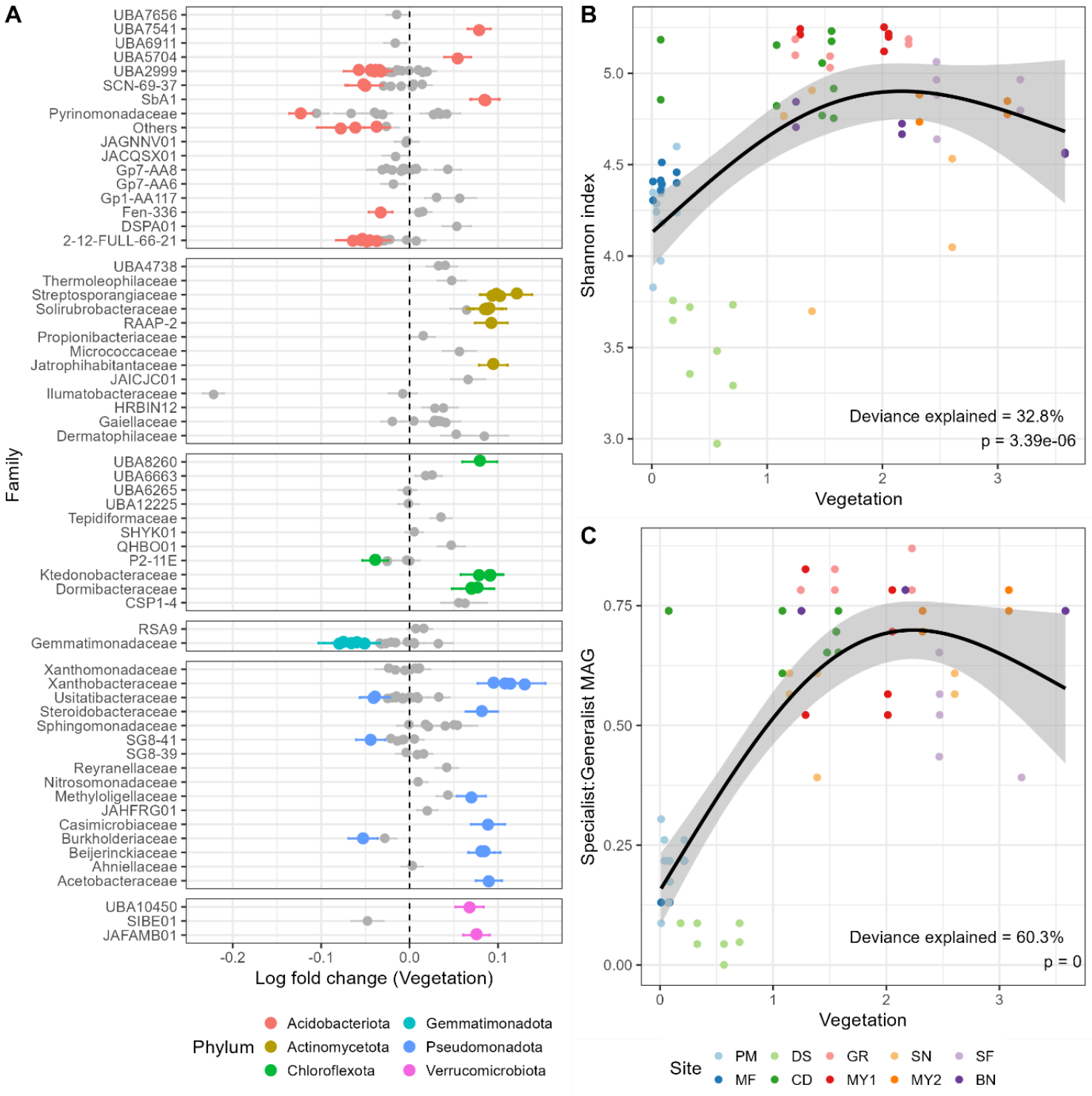


Figure 4

Vegetation impact on alpha diversity, specialist:generalist, and taxonomical abundance. A) Differential abundance analysis of MAGs with vegetation cover as predictor variable. Taxonomic names are on family level. Only significant MAGs are shown in color (diff_robust and passed_ss = TRUE), see Supplementary file S15. Generalized additive models (GAMs) of B) Shannon index (alpha diversity), C) the ratio of the number of specialist MAGs to the number of generalist MAGs (specialist:generalist MAG)

with vegetation cover as a predictor variable (log1p(x) transformed). See Supplementary file S16 - S18 for more information on GAMs.

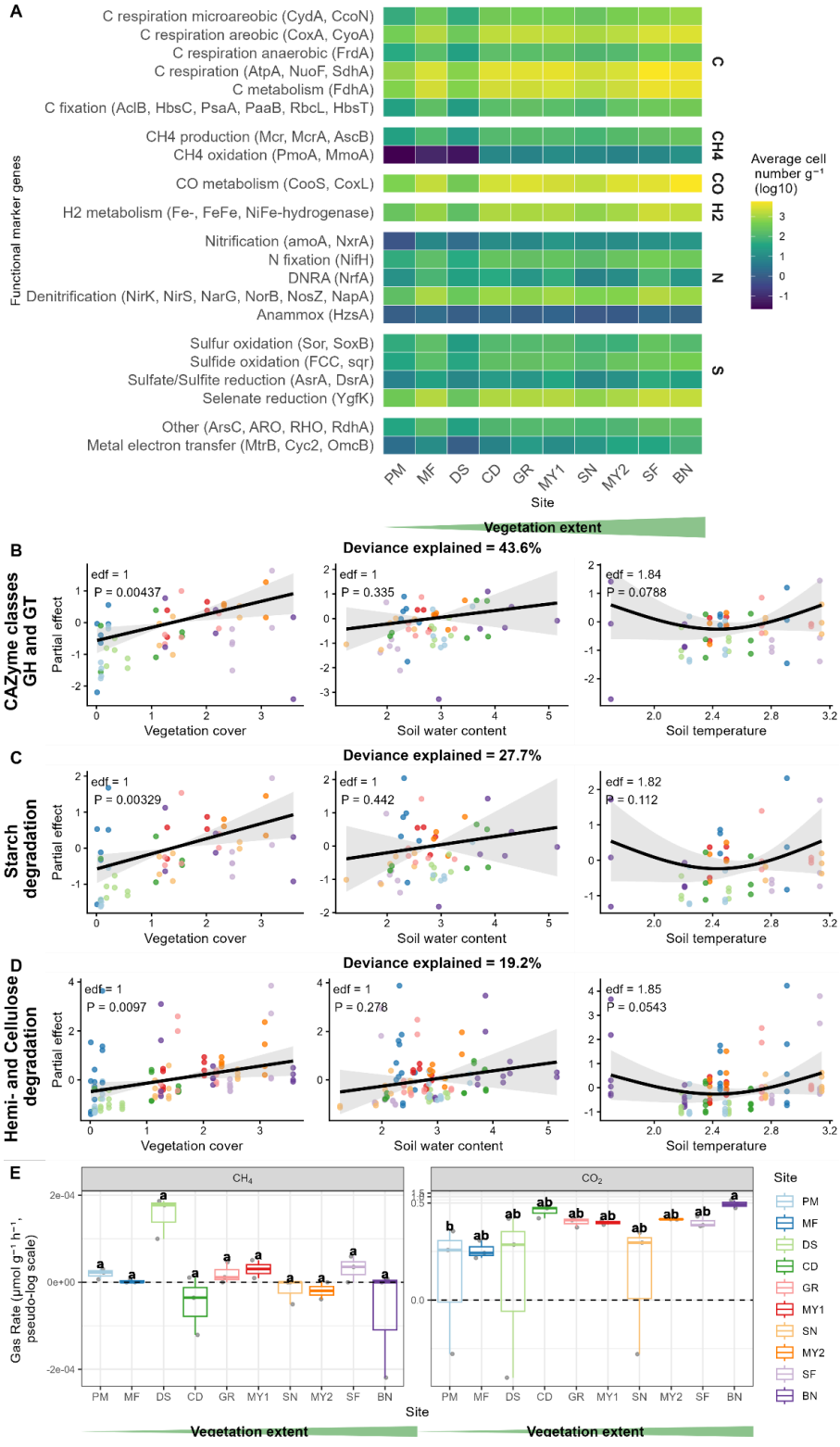


Figure 5

Functional genetic potential of the ten alpine permafrost-affected soils. A) Heatmap of functional gene abundances of C, N, S and trace gas cycling marker gene abundance across sites. Generalized additive

models (GAMs) of functional gene abundance of carbohydrate active enzyme (CAZymes) B) classes glycoside hydrolases (GH) and glycosyltransferases (GF), C) starch degradation and D) cellulose and hemicellulose degradation with vegetation cover, soil water content (SWC) and soil temperature as predictor variables and site as random effect. E) Gas rates for CH_4 and CO_2 from soil microcosms after 72h at 12.5°C (average sampling temperature). See Supplementary file S19 – S25 for more information on GAMs and statistical tests.

Supplementary Files

This is a list of supplementary files associated with this preprint. Click to download.

- AlpineSoils23Supplementaryfile.xlsx
- AlpineSoil23Supplementarymaterials.docx